Science of the Total Environment 737 (2020) 139535

Contents lists available at ScienceDirect

Science of the Total Environment

journal homepage: www.elsevier.com/locate/scitotenv

Overall comparison and source identification of PAHs in the sediments of European Baltic and North Seas, Chinese Bohai and Yellow Seas

Pu Wang [a,b,c], Wenying Mi [d], Zhiyong Xie [c,*], Jianhui Tang [e], Christina Apel [c], Hanna Joerss [c], Ralf Ebinghaus [c], Qinghua Zhang [b,a]

[a] Hubei Key Laboratory of Environmental and Health Effects of Persistent Toxic Substances, Institute of Environment and Health, Jianghan University, Wuhan 430056, China
[b] State Key Laboratory of Environmental Chemistry and Ecotoxicology, Research Center for Eco-Environmental Sciences, Chinese Academy of Sciences, Beijing 100085, China
[c] Institute of Coastal Research, Helmholtz-Zentrum Geesthacht, Geesthacht 21502, Germany
[d] MINJIE Institute of Environmental Science and Health Research, Geesthacht 21502, Germany
[e] Yantai Institute of Coastal Zone Research, Chinese Academy of Sciences, Yantai 264003, China

HIGHLIGHTS

- Relatively higher level of PAHs was observed in the Baltic Sea.
- PAHs in the European seas revealed the effect of proximity from source.
- Spatial distribution in the Chinese seas closely related to the hydrodynamic effect.
- Ratio of naphthalene against its methylated derivatives may indicate PAH sources.

GRAPHICAL ABSTRACT

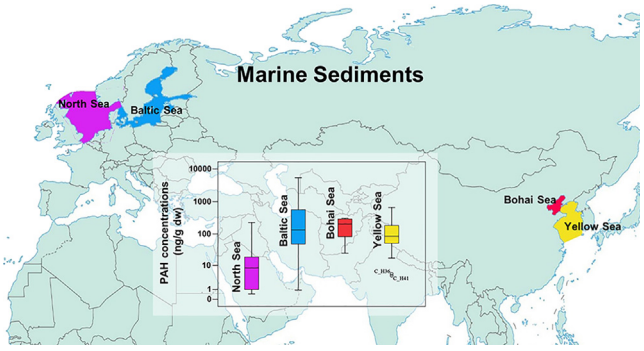

ARTICLE INFO

Article history:
Received 29 March 2020
Received in revised form 11 May 2020
Accepted 16 May 2020
Available online 29 May 2020

Editor: Jay Gan

Keywords:
Polycyclic aromatic hydrocarbons
Marine sediment
Baltic Sea
North Sea
Bohai Sea
Yellow Sea

ABSTRACT

An international sampling campaign was carried out to comprehensively investigate the occurrence of polycyclic aromatic hydrocarbons (PAHs) in the marine sediments from the European Baltic and North Seas, Chinese Bohai and Yellow Seas. The concentrations of $\sum_{18}$PAHs in the samples from these four seas were in the range of 0.91–5361 ng/g dry weight (dw), 0.46–227 ng/g dw, 25.0–308 ng/g dw and 4.3–659 ng/g dw, respectively. 4-rings PAHs, e.g., fluoranthene, pyrene and benzo(*b*)fluoranthene, were commonly the dominant compounds in all the samples. The PAH sources were identified via composition patterns, diagnostic ratios, principal component analysis (PCA) and positive matrix factorization (PMF). Coal combustion, vehicular emission, coke plant and petroleum residue were apportioned as the main sources in these marine sediments. However, through PMF modeling, different contributions of these sources were quantified to the deposited PAHs in the seas, suggesting distinct anthropogenic impacts on the adjacent marine system. It is note-worthy that biomass combustion may not be the main source of PAHs in the majority of sediments from these seas. This was evidenced by the ratios of naphthalene against its methylated derivatives (i.e. 1-,2-methylnaphthalenes) other than the composition pattern in the samples, of which the approach is in prospect of developing in future studies.

* Corresponding author at: Helmholtz-Zentrum Geesthacht, Centre for Materials and Coastal Research, Institute of Coastal Research, Geesthacht 21502, Germany.
E-mail address: zhiyong.xie@hzg.de (Z. Xie).

https://doi.org/10.1016/j.scitotenv.2020.139535
0048-9697/

1. Introduction

With the globally expanding economic and industrial developments in the 20th century, many developed and developing countries, such as the United Kingdom, USA, Japan and China, have experienced various environmental problems, including air, water, and soil pollution, even the food contamination, which raised great concerns about the environmental safety and local human health. Thereafter, energetic efforts have been made and significant improvements were achieved for the environment and human life in those developed countries. As two of the largest economy groups in the world, European Union (EU) and China have been experiencing different stages of the economic development in recent years. For example, Germany, the largest economy in EU, has established the mature industrial system with relatively less contamination, by contrast, many industries with severe pollution are still situated in China, which results in relatively higher emission of various pollutants in the environment including the surrounding marine system.

As typical bordering seas and semi-enclosed seas in the world (Fig. S1), the European Baltic and North Seas, and the Chinese Bohai and Yellow Seas have their societal significance with a broad range of important modes of uses, from oil and gas, nearshore aquaculture, offshore fishery, wind energy, shipping and other industrial activities to tourism and natural preservation. However, they also serve, or served, as dumping sites for onshore activities. A difference is the fact that the North European seas have many different national coasts while in case of the Chinese seas only a limited number of international partners share responsibility for the marginal seas. This possibly makes the pollution by anthropogenic activities of difference in these seas. Among the pollutants, persistent toxic substances (PTSs) received great attention due to their toxicity, persistence and bioaccumulation in the environment in the past several decades (Porta, 2015; Wang et al., 2017). Many PTSs are released from the terrestrial sources and may enter into the marine environment via long-range transport by water and/or air, leading to a potential exposure risk of the marine animals to various toxic chemicals (Wolska et al., 2012). Since most PTSs are hydrophobic and tend to bind strongly to particulate matter, which facilitates their deposition in water, sediment is therefore considered a primary reservoir of PTSs in aquatic systems (Maletić et al., 2019). Polycyclic aromatic hydrocarbons (PAHs) are such a kind of PTSs, which are known carcinogens and mutagens, and their sources, transport, and effects have been studied extensively (Kim et al., 2013). PAHs are natural components of coal and oil, and also formed during the combustion of fossil fuels and organic material, as well as biomass burning (Kim et al., 2013). They enter the marine environment through atmospheric deposition, road run-off, industrial discharges and oil spills (CEMP, 2009). PAHs sorbed on sediment are considered to be stabilized by physicochemical association with the sediment matrix, and undergo practically no further changes (Maletić et al., 2019). Therefore, its occurrence and distribution pattern in the marine sediment may provide important information for comparison of the impact from the anthropogenic activities on the adjacent marine system (Wolska et al., 2012; Maletić et al., 2019).

Even though the occurrence of PAHs in the marine environment was constantly studied in many coastal or oceanic areas (Maletić et al., 2019) including the European seas (CEMP, 2009) and Chinese seas (Zhao et al., 2020), less was done to comprehensively compare their distribution pattern and source composition in the marine sediment from different seas, which may limit the understanding of environmental fate of PAHs and anthropogenic effects on marine system on a global scale.

In the present study, an international sampling campaign was conducted on these four seas to comprehensively investigate occurrence of PAHs in the surface sediments. The potential sources were identified based on the composition patterns, diagnostic ratios, principal component analysis (PCA) and positive matrix factorization (PMF), and the quantitative comparison between the different areas may shed light on the fate of PAHs in the marine environment and anthropogenic impact from the surrounding countries.

2. Materials and methods

2.1. Sampling areas

The Baltic Sea is a relatively shallow inland sea in north-east Europe, bounded by the coastlines of Denmark, Estonia, Finland, Germany, Latvia, Lithuania, Poland, Russian Federation and Sweden (Fig. 1;

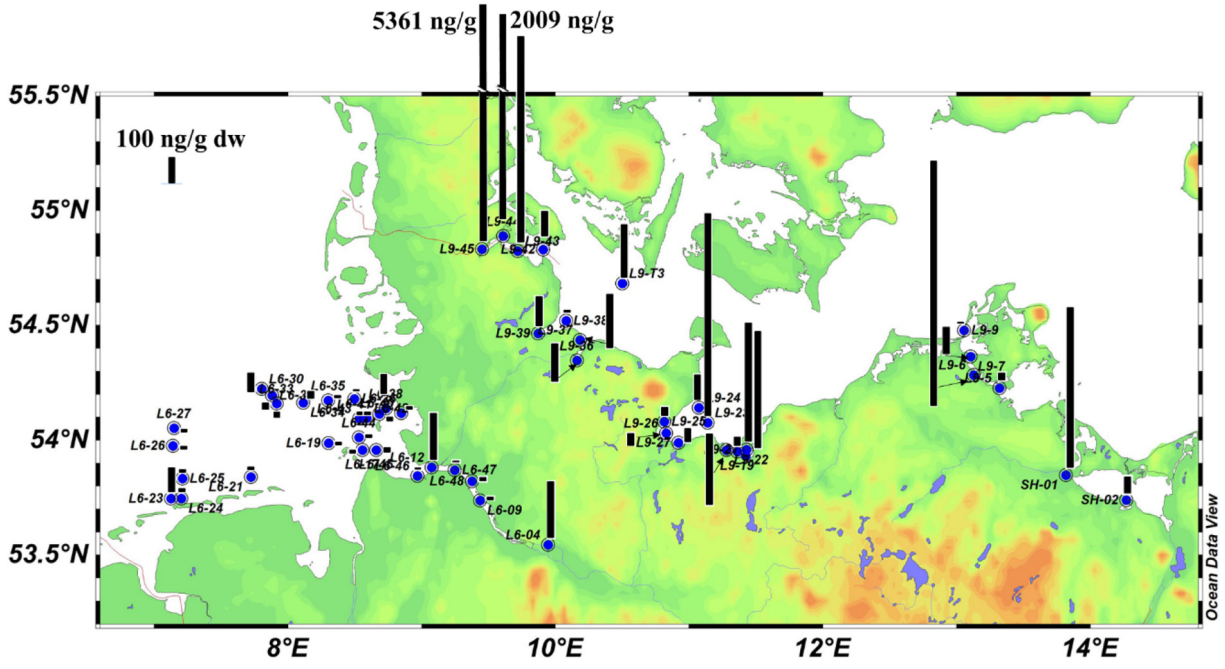

Fig. 1. The sampling locations and spatial distribution of $\sum_{18}$PAHs in the sediments from the Baltic Sea and North Sea.

Fig. S1). Its average depth is 57 m. As a semi-enclosed sea, the Baltic Sea received much runoff from coastal and river areas with high concentrations of population and industry, and has been recognized as an ecologically vulnerable system (Johannesson and Andre, 2006). The shallow sounds between Sweden and Denmark provide a limited water exchange with the North Sea. The North Sea is located in the northeastern arm of the Atlantic Ocean, and between the British Isles and the mainland of northwestern Europe (Fig. 1; Fig. S1). It serves as a prominent shipping zone among European countries and between Europe and the Middle East. A third aspect of economic importance has been the extensive reserves of petroleum and natural gas discovered beneath the seafloor. Few parts of the North Sea are >90 m in depth.

The Bohai and Yellow Seas are semi-enclosed marginal seas in the northwest Pacific Ocean, and some of the most extensive shelf seas in the world (Fig. S1). The Bohai Sea is surrounded by the Bohai Economical Rim (BER), which is the largest economic engine in North China. The Bohai Sea has an area of approximately 77,000 km^2 and an average depth of 18 m (Song et al., 2014). It received many fluvial sediments especially from Yellow river, and nearly 30% of the Yellow River-derived sediment has been ultimately transported out of the Bohai Sea into the Yellow Sea (Yang and Liu, 2007). The Yellow Sea is surrounded by the west coast of the Korean Peninsula and the east coast of China. It is connected to the Bohai Sea through the Bohai Strait, and its northern extension is referred to Korea Bay. The Yellow Sea has an area of approximately 380,000 km^2 and an average depth of 44 m (Song et al., 2014).

2.2. Sample collection

A total of 101 surface sediment samples were collected from the four different seas, including 24 from the Baltic Sea, 27 from the North Sea (including 6 from the river Elbe Estuary, Germany) (Fig. 1), 11 from the Bohai Sea and 39 from the Yellow Sea (Fig. 2). The samples in the German Bight of the North Sea and Germany Baltic Sea coastline were collected on the research vessel *Ludwig Prandtl* in June and September 2017, respectively. While on the sampling campaign in the Chinese Bohai and Yellow Seas, the surface sediment samples were collected on the Chinese research vessel *Dongfanghong* 2 in June and July 2016, where a gridded sampling strategy was carried out. Stainless-steel box corers were used and the top 10 cm of sediment was taken on both the sampling campaigns. The samples were put afterward into the aluminum bowls (pre-cleaned with acetone and baked out at 250 °C) and stored at −20 °C until sample pretreatment.

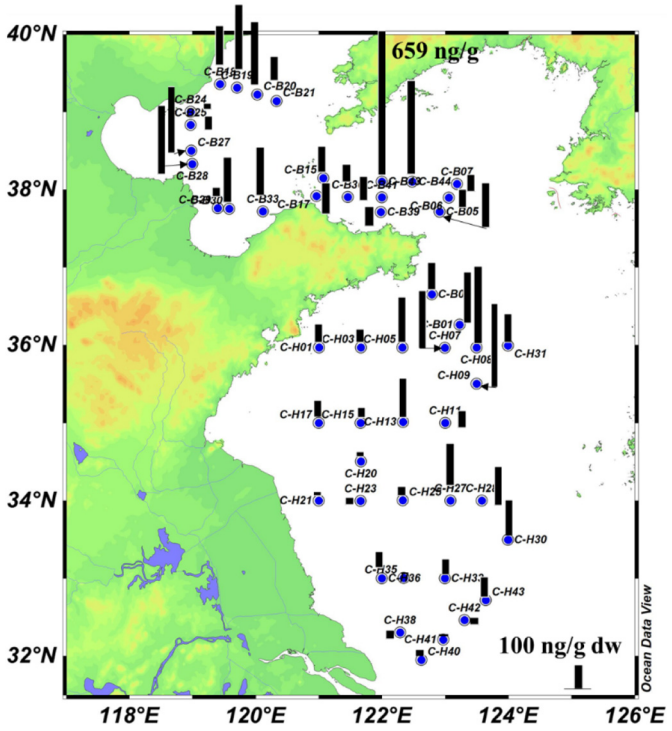

Fig. 2. The sampling locations and spatial distribution of $\sum_{18}$PAHs in the sediments from the Bohai Sea and Yellow Sea.

2.3. Sample extraction, cleanup and instrumental analysis

The details about sample extraction, cleanup procedures and instrumental analysis were given in the *Supplementary materials*. Briefly, the frozen sediment samples were freeze-dried, homogenized and then extracted by Ultrasonic assisted extraction. The extract was cleaned up through a silica gel column and finally concentrated for instrumental analysis. PAH analysis was performed on a gas chromatograph/mass spectrometer (GC/MS) (Agilent 6890N GC/5973N MSD, USA), and 16 US EPA priority PAHs and 2 methylnaphthalenes (1- and 2-MN) were measured (Table S1).

2.4. Quality assurance/quality control (QA/QC)

16 deuterated internal standards (d-PAHs) were spiked in the samples for qualification and quantification, and ^{13}C-labeled PCB-208 was added for recovery calculation. The average recoveries were 87 ± 27% in all the samples. The procedural (laboratory) blank was processed for each batch of 10 samples. Method detection limits (MDLs) were calculated as average blank plus three times standard deviation (SD) of the targets in the procedural blanks, and the values were in the range of 0.003–0.04 ng/g (Table S1).

3. Results and discussion

3.1. The overall concentrations and distribution

The sum concentrations of 18 PAHs ($\sum_{18}$PAHs, including 1- and 2-MN) were in the range of 0.91–5361 ng/g dry weight (dw) with a mean of 549 ± 1124 ng/g dw in the sediments from the Baltic Sea, while they were in the range of 0.46–227 ng/g dw (mean 30.2 ± 57.2 ng/g dw), 25.0–308 ng/g dw (mean 184 ± 109 ng/g dw) and 4.3–659 ng/g dw (mean 138 ± 133 ng/g dw) in the North Sea, Bohai Sea and Yellow Sea, respectively (see Table 1). Relatively higher level was observed in the Baltic Sea, which may be attributed to the fact that most of the sampling sites were in close proximity to land and/or in bays or estuaries, and revealed the effect of proximity from source. Even so, they were generally comparable to those reported in the previous studies (Baumard et al., 1999; Ricking and Schulz, 2002; SRU, 2004) (Table S2). The two highest values were obtained in the sampling sites L9–44 (2009 ng/g dw) and L9–45 (5361 ng/g dw), both of which were located in the Flensburg Fjord, the northern end of Germany (Fig. 1). The main industries in Flensburg are shipbuilding, metal processing and paper making, which may lead to elevated emission of PAHs into the water system. On the other hand, the Flensburg Fjord is semi-enclosed with low water exchange rate against the Baltic Sea, probably increasing the deposition of PAHs into sediment. Higher concentrations were also found in the sites L9–6 (998 ng/g dw), and L9–20/21 (471/480 ng/g dw), which were nearby the port cities of Stralsund and Wismar, respectively. Furthermore, relatively higher concentration was observed in the site SH-01 (648 ng/g dw), which was located at the Peene River Estuary, Germany.

In the North Sea, the PAH concentrations in sediment were generally lower than those from the other three seas, but comparable to the monitoring data from the convention for the Protection of the Marine Environment of the North-East Atlantic (OSPAR) over the period of 2010–2015 (OSPAR, 2017). Whereas, they were lower than those in a special report by the German Advisory Council on the Environment in

Table 1
The concentrations of PAHs (ng/g dw) and other parameters in the sediments from the Baltic Sea, North Sea, Bohai Sea and Yellow Sea.

Compound	Baltic Sea (n = 24)			North Sea (n = 27)			Bohai Sea (n = 11)			Yellow Sea (n = 39)		
	Range	Mean ± SD	Median	Range	Mean ± SD	Median	Range	Mean ± SD	Median	Range	Mean ± SD	Median
NaP	0.02–16.4	1.21 ± 3.30	0.36	0.02–2.91	0.45 ± 0.75	0.16	1.04–14.1	5.17 ± 3.78	3.99	0.45–17.6	3.75 ± 2.92	2.84
2-MN	0.01–10.2	0.98 ± 2.11	0.34	0.01–2.84	0.49 ± 0.79	0.14	0.70–11.0	4.69 ± 3.04	4.22	0.22–19.4	3.15 ± 3.20	2.34
1-MN	0.008–6.60	0.68 ± 1.41	0.25	0.006–1.79	0.32 ± 0.50	0.09	0.41–5.82	2.65 ± 1.64	2.47	0.09–11.4	1.83 ± 1.89	1.34
Acy	0.01–20.1	2.79 ± 5.52	0.46	0.006–1.72	0.16 ± 0.39	0.03	0.04–1.01	0.37 ± 0.29	0.31	<MDL-1.44	0.23 ± 0.27	0.13
Ace	<MDL-10.0	1.09 ± 2.49	0.23	0.005–0.94	0.13 ± 0.22	0.03	0.06–1.62	0.61 ± 0.46	0.42	0.01–3.83	0.33 ± 0.61	0.17
Flu	0.009–47.7	3.49 ± 9.94	0.68	0.007–2.49	0.36 ± 0.66	0.07	0.38–5.21	2.42 ± 1.55	2.40	0.05–9.77	1.40 ± 1.67	0.93
Phe	0.03–497	30.3 ± 100.1	6.40	0.03–14.4	1.92 ± 3.32	0.47	1.84–23.4	13.6 ± 7.8	14.2	0.26–42.9	9.77 ± 9.44	6.39
Ant	0.009–28.1	3.94 ± 6.82	1.16	<MDL-3.19	0.43 ± 0.82	0.12	0.21–3.02	1.63 ± 1.00	1.95	0.01–6.16	0.91 ± 1.11	0.57
Fla	0.07–1663	117 ± 336	23.4	0.04–40.7	4.70 ± 9.65	1.01	3.76–56.9	32.8 ± 20.1	35.3	0.39–97.7	19.6 ± 19.9	13.6
Pyr	0.11–970	92.2 ± 204.8	21.5	0.04–37.5	4.33 ± 8.96	1.01	2.83–41.1	23.4 ± 14.2	25.5	0.32–71.2	13.6 ± 14.0	8.54
BaA	0.06–324	35.2 ± 69.9	9.30	0.02–15.7	1.75 ± 3.67	0.34	0.88–13.4	7.68 ± 4.89	7.96	0.07–27.6	4.83 ± 5.45	2.71
Chr	0.07–472	50.6 ± 102.1	12.9	0.03–24.4	3.15 ± 6.50	0.71	2.61–32.1	19.5 ± 11.6	22.2	0.37–65.1	15.0 ± 14.6	9.47
BbF	0.10–432	57.8 ± 105.3	15.2	0.04–18.9	2.97 ± 5.23	0.75	3.01–38.2	21.6 ± 13.3	22.3	0.66–79.1	19.4 ± 17.9	12.6
BkF	0.08–297	44.2 ± 74.0	11.0	0.02–20.9	2.54 ± 5.37	0.52	1.76–18.1	10.7 ± 6.1	10.6	0.35–48.1	10.5 ± 9.8	7.49
BaP	0.05–279	40.1 ± 71.9	11.3	0.01–17.5	2.24 ± 4.43	0.38	1.22–16.9	9.68 ± 6.09	9.29	0.07–37.6	6.08 ± 6.97	3.66
InP	0.10–120	28.9 ± 34.3	15.1	0.04–15.0	2.57 ± 4.40	0.57	1.80–21.3	12.1 ± 7.4	11.9	0.24–51.1	12.9 ± 12.3	7.78
DBA	0.02–26.9	5.76 ± 7.12	2.76	<MDL-3.77	0.52 ± 0.99	0.11	0.28–2.85	1.55 ± 0.97	1.75	0.02–9.64	1.82 ± 1.89	1.32
BghiP	0.08–248	32.8 ± 55.7	12.0	0.01–5.83	1.16 ± 1.74	0.40	2.14–23.7	13.9 ± 8.3	14.1	0.47–59.5	13.2 ± 12.8	7.82
Σ_{18}PAHs	0.91–5361	549 ± 1124	135	0.46–227	30.2 ± 57.2	8.13	25.0–308	184 ± 109	204	4.3–659	138 ± 133	85.3
TOC (%)	0.05–6.13	2.16 ± 1.77	2.13	0.01–6.00	0.59 ± 1.20	0.13	0.10–1.20	0.59 ± 0.39	0.63	0.06–1.30	0.53 ± 0.37	0.42
Water temperature (°C)	17.2–19.8	18.3 ± 0.8	18.1	13.5–21.1	16.4 ± 1.9	16.2	5.3–9.6	7.0 ± 1.6	6.5	5.5–11.2	8.5 ± 1.8	8.9
Depth (m)	2.0–25.0	12.1 ± 7.8	11.0	1.8–40.8	32.6 ± 11.9	37.3	14.5–29.0	21.6 ± 4.5	22.0	15.0–80.0	46.1 ± 20.5	40.7
Salinity (‰)	1.1–18.0	12.3 ± 4.6	12.1	0.6–33.2	24.7 ± 10.9	28.7	31.2–32.3	31.9 ± 0.4	32.1	30.1–33.8	32.3 ± 0.7	32.3
pH value	7.88–8.76	8.25 ± 0.18	8.23	7.75–8.25	8.10 ± 0.17	8.19						

2004 (SRU, 2004) and those from the river Elbe Estuary, Germany (260–906 ng/g dw) (Otte et al., 2013) (Table S2). The two highest concentrations were obtained from the sites L6–04 (227 ng/g dw) and L6–12 (187 ng/g dw), which were situated along the river Elbe and close to the Hamburg harbor and the Kiel Canal Estuary, respectively (Fig. 1). Moreover, higher concentrations were found in the sites L6–23 (96.3 ng/g dw) and L6–30 (74.3 ng/g dw), which were close to the islands of tourist attraction nearby Netherlands.

In the Chinese seas, the PAH concentrations in the sediments from the Bohai Sea were generally higher than those from the Yellow Sea, and those in the north Yellow Sea were higher than in the south part (Fig. 2). Furthermore, PAHs showed an increasing tendency along the distance from the coastline toward the open sea, which was consistent with the previous observations (Lin et al., 2011; Li et al., 2015; Lin et al., 2017), as well as some other organic pollutants in this area (Apel et al., 2018; Mi et al., 2019). The fluvial sediments are transported, deposited and redistributed, forming coarse-grained sand, fine-grained mud and sand-mud mixture deposits on the continental shelf under intense tidal, wave and coastal conditions in the east China seas. (Yang and Liu, 2007; Qiao et al., 2017), However, all of the coastal currents generally flow southwards and warm currents enter northwards, resulting in the mud deposit areas located off the Yellow River and in the central Bohai Sea, around the end of the Shandong Peninsula, and in the central South Yellow Sea (Qiao et al., 2017). The higher PAH levels were commonly found in the mud deposit areas, which may reflect hydrodynamic effect on spatial distribution of the deposited PAHs (Qiao et al., 2017). The PAH levels in the Chinese seas were generally comparable to those reported in the same areas (Lin et al., 2011; Li et al., 2015; Lin et al., 2017; Xu et al., 2019) (Table S2). The highest concentration (659 ng/g dw) was observed in the site C—B43 in the north Yellow Sea, followed by the nearby site C—B44 (424 ng/g dw), both of which were in the mud deposit area close to the Shandong peninsula. This observation was consistent with the previous studies on the organic UV stabilizers and UV filters (Apel et al., 2018), as well as phthalate esters (Mi et al., 2019) in the same area.

3.2. PAH profiles in sediment

Regarding the PAH profiles, 4-rings PAHs, e.g., fluoranthene (Fla), pyrene (Pyr) and benzo(*b*)fluoranthene (BbF) were commonly dominant compounds in the samples from all the seas, accounting for 14.1%, 11.8% and 12.1% of $\sum_{18}$PAHs on average, respectively (Fig. S2). This profile was generally consistent with many previous studies in these seas (Li et al., 2015; Lin et al., 2017; OSPAR, 2017).

Specifically, in the European seas, indeno(1,2,3-*cd*)pyrene (InP) made relatively higher contributions with a percentage of 9.8% on average, especially in the site L6–24 (22%), which was close to the island of tourist attraction in the North Sea. For the individual site, relatively higher percentage of Fla. was observed in the sites L9–45 (31%) and L9–21 (25%) in the Baltic Sea. Moreover, although the levels of naphthalene (NaP) and its alkylated derivatives (1- and 2-MNs) were relatively low in the sites L6–17/19/21/36 in the North Sea (<133 ng/g dw), they contributed evidently high with a sum percentage of about 20% $\sum_{18}$PAHs in each site, indicating a source characteristic of petrogenic origin (Yang et al., 2017).

In the Bohai and Yellow Seas, chrysene (Chr) generally accounted for higher percentages (mean 10.5%). This was different from the results by Li et al. (Li et al., 2015) and Lin et al. (Lin et al., 2017), where phenanthrene (Phe) was found as one of dominant compounds other than 4-rings PAHs. Furthermore, NaP showed relatively higher contributions (over 6.5%) in the sites C-H20/21/23, C-H35/36 and C—H41, as well as 1- and 2-MNs. These sites were generally close to the coastline of Jiangsu province, where highly developed manufacturing and shipping industries were located. The higher contribution of NaP and its methylated derivatives may therefore relate to the industrial emission in this area (ATSDR, 2005).

PCA was employed to further explore the PAHs distribution characteristic among the different seas. As exhibited in Fig. S3, 85.5% of the PAHs variation could be explained by PC1 (70.4%) and PC2 (15.1%) (Eigenvalue >1). PC1 was characterized by the US EPA priority PAHs without NaP, while PC2 was featured by NaP and its methylated derivatives, i.e. 1- and 2-MNs. Regarding the score plot, L9–45, −44, and C—B43 were distinctively separated from the others. As mentioned above, both the sites L9–44 and −45 were located in the Flensburg Fjord, where much complex sources exist and may lead to different contamination characteristics from the others. Whereas, the site C—B43 was in the mud deposit area close to the Shandong peninsula, which probably induced the distinct distribution profile of PAHs in the adjacent marine system.

3.3. The effect of total organic carbon (TOC) and other parameters

TOC is considered an important factor to influence the distribution of organic contaminants in solid matrix (Cornelissen et al., 2005). In this study, the TOC contents were generally low in the sediments (Table 1), while a relatively higher level was obtained from the Baltic Sea ($p < 0.01$). This may be expected because of the sampling sites in close proximity to land and/or in bays or estuaries in this intracontinental sea. Significantly positive dependence was found for the PAH concentrations against TOC contents (Spearman coefficient = 0.754, $p < 0.01$), and higher R^2 values were obtained for the linear regressions in the Bohai Sea and Yellow Sea (Fig. S4). This may be ascribed to that the sampling sites were griddedin the mud deposit area and the adsorption of pollutants was mainly driven by TOC, which was also reported in the previous studies (Lin et al., 2017; Xu et al., 2019).

The relationships between the PAH concentrations and other parameters were also explored, including water temperature, salinity, pH value (only obtained in the European seas) and depth of the sampling site. Significantly positive correlation was only obtained against the depth in the Yellow Sea ($p < 0.001$) (Fig. S5), which was in well agreement with the increasing tendency of PAH and TOC levels along the distance from the coastline toward the open sea, and confirmed the hydrodynamic effect on spatial distribution of the deposited PAHs.

3.4. Source identification

PAHs encompass both parent (non-alkylated) compounds and alkylated homologues. Although PAHs can be produced through natural processes, they also arise from anthropogenic sources. Various combustion processes are the major source of PAHs, commonly comprising the heavier, parent (non-alkylated) PAHs, whereas they can also be of petrogenic origin (crude oils or refinery products) with mainly alkylated, 2–3 rings PAHs formed as a result of diagenetic processes.

The 16 US EPA priority PAHs were grouped into 2–3 rings low-molecular weight (LMW) and 4–6 rings high-molecular weight (HMW) PAHs, and the LMW/HMW ratio was generally employed for primary evaluation of PAH sources. In the present study, this ratio ranged from 0.08–0.81 in all the samples, suggesting a common source of pyrolytic origin. It was generally in agreement with previous studies in these seas (Lin et al., 2011; Jiao et al., 2012; Tobiszewski and Namieśnik, 2012; Louvado et al., 2015; Wang et al., 2015). One-way ANOVA analysis (Tukey HSD) indicated that significant higher ratios were obtained from the North Sea compared with those from the Baltic Sea and Yellow Sea ($p \le 0.001$). Whereas, for the individual site, only several higher ratios (>0.5) were observed in the sites such as L6–17/19/25/32/33/36/48 in the North Sea and C-H20/21 in the Yellow Sea. These higher ratios of LMW PAHs may stem from fossil fuel (such as diesel) spillage from ships and boats, other than lower temperature combustion (Mai et al., 2003), implying possible source of petrogenic origin in the North Sea (OSPAR, 2010) and some locations in the other seas.

Furthermore, diagnostic ratios of marker species were calculated. The majority of Fla./(Fla + Pyr) and InP/(InP+ benzo(g,h,i)-perylene (BghiP)) ratios were >0.5 (Fig. 3), indicating pyrogenic source of biomass and coal combustion in most of the sampling sites (Guo et al., 2006). Some of these ratios were <0.5, but still higher than the threshold values of petrogenic origin, declaring the contribution from petroleum combustion. On the other hand, the lower benzo(*a*)anthracene (BaA)/(BaA + Chr) and anthracene (Ant)/(Ant+Phe) ratios ostensibly implied that PAHs in some sites especially the Chinese seas could be of petrogenic origin (Guo et al., 2006). Previous studies indicated that Ant and BaA have higher potential of photolysis than Phe and Chr, which made diagnostic ratios of BaA/(BaA + Chr) and Ant/(Ant+Phe) questionable during long range transport of PAHs (Yan et al., 2005; Deng et al., 2013; Lin et al., 2017). Despite that, river discharge and the coastal currents flowing southwards contributed much to the sediment in the two Chinese seas, and the sampling sites in the European seas were mainly along the coastlines. Therefore, the ratios of BaA/(BaA + Chr) and Ant/(Ant+Phe) could to large extent distinguish PAH sources in the different seas. As exhibited in Fig. 3, the ratios from the Chinese seas were generally clustered together, while those from the Baltic and North Seas were more scattered, suggesting some distinct source characteristics between them. This phenomenon could also be observed by PCA analysis when using these ratios as variables (Fig. S6), where the sampling sites in the Baltic Sea were characterized by BaA/(BaA + Chr), Ant/(Ant+Phe) and InP/(InP + GghiP), while those in the North Sea were featured by ∑LMW/∑HMW other than them. This further indicated discrepancy in the PAH sources between the two European seas, probably due to the effect of proximity from source, while similar sources in the two Chinese seas because of hydrodynamic effect.

NaP and its methylated derivatives are not only the natural constituents of mineral oil, but also produced commercially. They are also unintentionally discharged during the burning of wood or tobacco, and

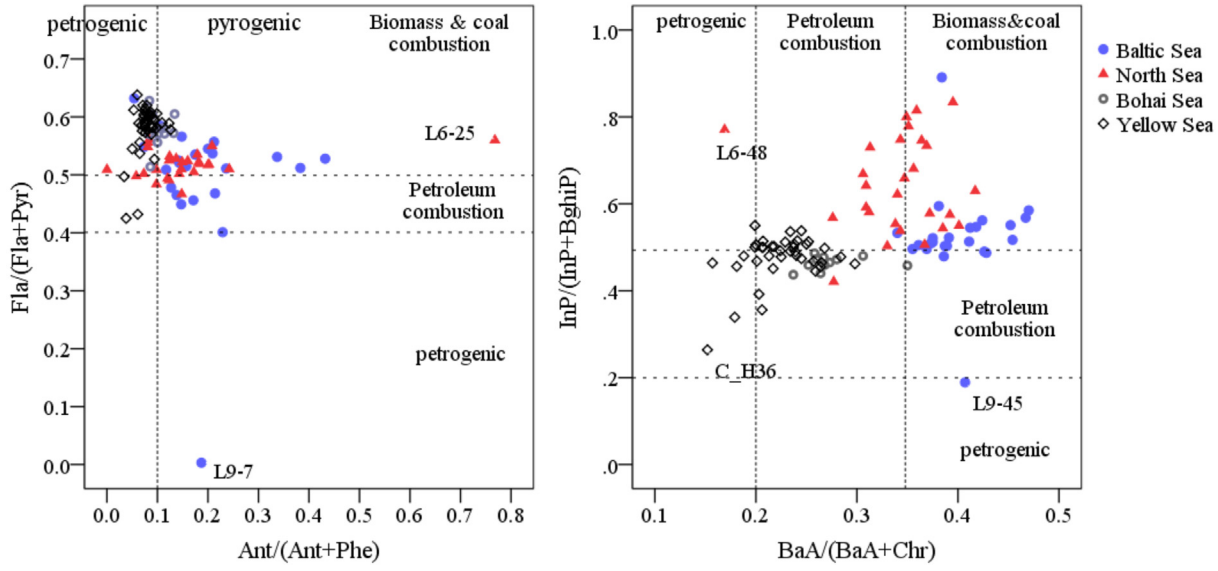

Fig. 3. The diagnostic ratios of PAHs in the sediments: (A) Fla./(Fla + Pyr) versus Ant/(Ant+Phe); (B) InP/(InP + GghiP) versus BaA/(BaA + Chr).

accidental spills (ATSDR, 2005). Whereas, little was reported about environmental fate of the methylated derivatives, i.e. 1- and 2-MNs (ATSDR, 2005). In this case, the composition of NaP and its methylated derivatives in the samples may provide information for the source identification. As Conde et al. (Conde et al., 2005) indicated, PAHs emission from combustion of agricultural and sylvicultural debris (i.e. biomass) were dominated by NaP, 2-MN, 1-MN, Phe and acenaphthylene (Acy), and the ratios normalized to NaP were about 0.4, 0.3, 0.25 and 0.2, respectively. Jenkins et al. (Jenkins et al., 1996) also found a signature of NaP and Phe during various biomass combustion, and almost all the ratios of 2-MN/NaP were lower than 0.5. While for the PAHs of petrogenic origin, the ratios of 1-MN/2-MN in the Bakken crude oils, diesel and gasoline samples were lower than 0.75 as Yang et al. (Yang et al., 2017) investigated, Soliman et al. (Soliman et al., 2014) also obtained that the ratios of 2-MN/NaP and 1-MN/NaP was 0.58 and 0.36 on average in the Qatar coastal sediments, and 0.62 for 1-MN/2-MN as expected. In the present study, there were significant correlations between the concentrations of 1−/2-MNs and NaP in all the seas ($p < 0.001$), and the ratios of 2-MN/NaP and 1-MN/NaP (slope of the regression line) were about 0.86 and 0.50, respectively (Fig. 4). The ratio of 1-MN/2-MN was expectedly 0.58, comparable to those of petrogenic source (Soliman et al., 2014; Yang et al., 2017), but obviously lower than 0.75 for biomass burning (Conde et al., 2005). Considering that Phe was not the dominant PAH compound in the sediments, it suggested that biomass combustion should not be the main source of PAHs in the majority of sampling sites, while petroleum residue may be ubiquitous in the European and Chinese seas. Regarding the site L9–45, the ratios of 2-MN/NaP and 1-MN/NaP were 1.32 and 1.18, resulting in a 1-MN/2-MN ratio of 0.89, distinctly higher than that from the nearby site L9–44 (0.65). Since L9–45 was characterized by the parent PAHs without NaP (Fig. S3), and Fla. and Pyr were the dominant compounds with lower concentrations of 5–6 rings PAHs, it suggested a source characteristic of coal combustion in this site (Levendis et al., 1998; Li et al., 2016). However, the site L-44 was featured by NaP and 1-, 2-MNs via PCA analysis, and benzo(*b*)fluoranthene (BbF), benzo(*k*)fluoranthene (BkF) and benzo(*a*)pyrene (BaP) accounted for a higher proportion, suggesting a contribution from vehicle emission (Li et al., 2016). This was also in agreement with the distribution characteristic in the site C—B43 from the Yellow Sea.

PMF was commonly utilized to estimate contribution of the specific PAH source categories (Lin et al., 2011; Tobiszewski and Namieśnik, 2012; Li et al., 2016; Maletić et al., 2019). Details about PMF modeling process could be found elsewhere (Lin et al., 2011; Norris et al., 2014; Li et al., 2016). In this study, an empirical uncertainty of 20% was adopted as an estimate of the confidence level based on the results from regularly analyzing the standard reference material (Mai et al., 2003; Lin et al., 2011). Taking the background of the PAH release sources in these seas into consideration, different factor (3, 4 and 5) and seed numbers (20, 50 and 100) were tested at first, and the solution with 4 factors and 50 seeds was selected to yield the most stable and interpretable results. Four typical PAH source profiles were finally selected referring to acknowledged references (Khalili et al., 1995; Levendis et al., 1998; Marr et al., 1999; Larsen and Baker, 2003; Liu et al., 2009; Li et al., 2016) to verify the source contribution from PMF modeling, including 1) vehicular emissions, 2) coal combustion, 3) petroleum residue, and 4) coke plant. In order to compare with the previous studies, PMF modeling was performed only for 16 US EPA priority PAHs. As shown in Fig. 5, each factor had a similar contribution in the samples from the Baltic Sea with a slightly higher proportion for coal combustion (29.8%). Whereas in the North Sea, coke plant was substantially largest in proportion (34.9%), followed by petroleum residue (28.6%) and vehicular emission (28.0%). Additionally, an unidentified source was quantified with a proportion of 8.6%. This profile may reflect a decline of the impact of offshore oil and gas development on the marine environment in recent years (OSPAR, 2010). However, in the Bohai Sea, a combined characteristic of coal combustion and vehicular emission was revealed with an evidently higher proportion (65.4%), followed by petroleum residue (16.7%). Analogously, a mixture contribution of coke plant and coal combustion accounted for 44.5% of the PAH levels in the samples from the Yellow Sea, while vehicular emission singly contributed to 29.7% of the deposited PAHs, followed by petroleum residue with a proportion of 15.2%. This was generally in accordance with the previous studies (Liu et al., 2009; Lin et al., 2017; Zhang et al., 2020). In addition, some unknown sources were also identified with the contributions of 10.8% and 7.1% in the Bohai Sea and 10.7% in the Yellow Sea, respectively, probably biomass combustion as considered previously (Lin et al., 2011; Deng et al., 2013; Lin et al., 2017; Zhang et al., 2020), suggesting complex source components in these two seas.

These modeling results were generally consistent with those from the diagnostic ratios. As shown in Fig. 3(A), even though the Fla./(Fla + Pyr) values were at the same level in the European seas, there were more ratios of Ant/(Ant+Phe) lower than 0.15 in the North Sea, suggesting more the sampling sites contaminated by PAHs of petrogenic origin. This was also in accordance with the results of ∑LMW/∑HMW, which was discussed previously. Similar situation was observed for BaA/(BaA + Chr) with more ratios between 0.2 and 0.35 in the North Sea (Fig. 3(B)), which indicated a common source of petroleum combustion, corresponding to higher contribution of vehicular emission in the North Sea than in the Baltic Sea (Fig. 5). On the other hand, the diagnostic ratios revealed very similar source patterns in the two Chinese seas, whereas, distinctive contributions from various sources were resolved from the PMF modeling in the Bohai and Yellow Seas, showing the advantage of this approach for source apportionment.

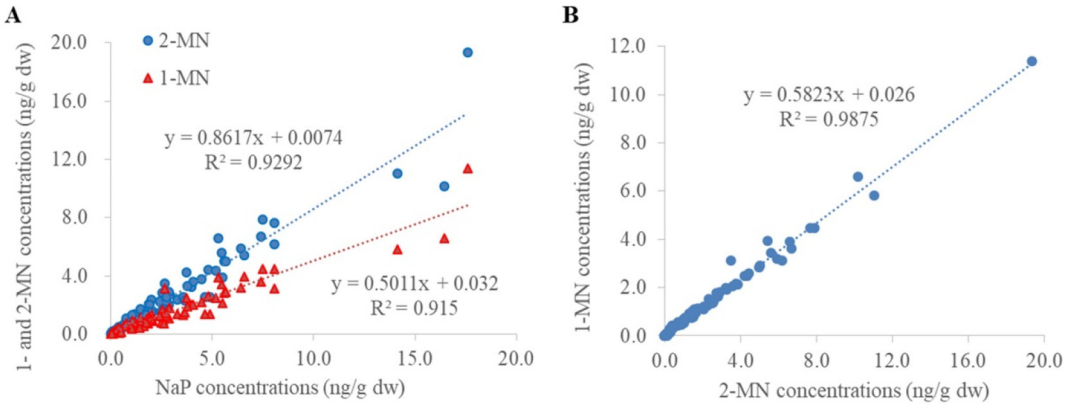

Fig. 4. The relationships between NaP and 1−/2-MNs (A), 1-MN and 2-MN (B) in the sediments from the different seas.

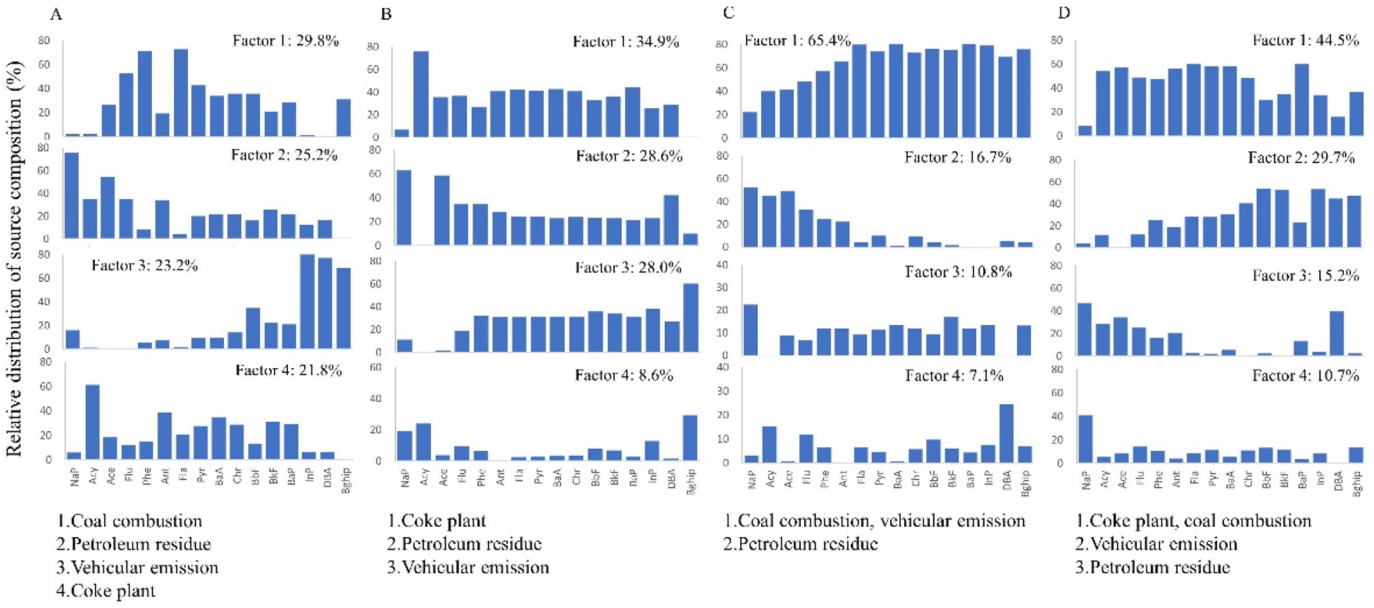

Fig. 5. The source profiles of PAHs derived from PMF modeling in the sediments from the four different seas (A: Baltic Sea; B: North Sea; C: Bohai Sea; D: Yellow Sea).

The results of source apportionment were generally consistent with the previous reports in the Chinese seas (Lin et al., 2011; Li et al., 2016) and the European seas (SRU, 2004; Lubecki and Kowalewska, 2010; OSPAR, 2010, 2017), where coal combustion, vehicular emission, petroleum residue and coke plant were commonly apportioned as the PAH sources. Whereas, limited data was available for their quantitative contributions in the marine sediments, especially in the European seas. In this case, the quantitative comparison between the different areas in the present study may shed light on the effect of proximity from source and hydrodynamic effect on spatial distribution of pollutants in the marine sediments.

4. Conclusions

In the present study, PAHs were intensively investigated in the sediments from four different seas including the European Baltic Sea and North Sea, Chinese Bohai Sea and Yellow Sea. Higher levels of $\sum_{18}$PAHs were detected in the Baltic Sea, while distinctly lower levels were measured in the North Sea. Combining with various approaches for source identification, coal combustion, petroleum residue, vehicular emission and coke plant were appointed as the main sources of PAHs in the surface sediments. Particularly, the ratios of NaP and its methylated derivatives (i.e. 1- and 2-MNs) evidenced that biomass combustion may not be the main source in the majority of sediments from these seas. This approach showed its great significance for source apportionment, and is in prospect of developing in the future study. Furthermore, different source contributions were quantified in the different seas, which may to some extent reflect the regional emission intensity of various PAH sources in the past decades.

One drawback is that, due to the limited tonnage of the research vessel *Ludwig Prandtl*, the majority of surface sediments from the European seas especially the Baltic Sea were obtained near the coastline, of which the results may reveal the effect of proximity from source. While the samples from the Chinese part were collected in the open sea because of the larger tonnage of *Dongfanghong* 2, of which the spatial distribution closely related to the hydrodynamic effect in this area. This may undervalue the quantitative comparison of source contributions in the different seas. More studies are warranted to further confirm the source contributions from the anthropogenic activities around these seas.

CRediT authorship contribution statement

Pu Wang: Writing - original draft, Methodology, Software, Formal analysis, Investigation, Data curation, Writing - review & editing, Visualization, Project administration, Funding acquisition.**Wenying Mi:**Methodology, Validation, Investigation.**Zhiyong Xie:**Conceptualization, Methodology, Investigation, Resources, Data curation, Writing - review & editing, Visualization, Supervision, Project administration, Funding acquisition.**Jianhui Tang:**Resources, Writing - review & editing, Funding acquisition.**Christina Apel:**Resources.**Hanna Joerss:**Resources.**Ralf Ebinghaus:**Writing - review & editing, Funding acquisition.**Qinghua Zhang:**Writing - review & editing, Funding acquisition.

Declaration of competing interest

The authors declare that they have no known competing financial interests or personal relationships that could have appeared to influence the work reported in this paper.

Acknowledgments

This study was jointly supported by the National Natural Science Foundation of China (41676183, 41977327 and 91743206), and German BMBF (03F0786C). We are grateful for the field assistance from the crew of Research Vessel *Dongfanghong 2* of the Ocean University of China and the crew of German Research vessel *Ludwig Prandtl*.

Appendix A. Supplementary data

Supplementary data to this article can be found online at https://doi.org/10.1016/j.scitotenv.2020.139535.

References

Apel, C., Tang, J., Ebinghaus, R., 2018. Environmental occurrence and distribution of organic UV stabilizers and UV filters in the sediment of Chinese Bohai and Yellow Seas. Environ. Pollut. 235, 85–94.

ATSDR, 2005. Public Health Statement for Naphthalene, 1-Methylnaphthalene, and 2-Methylnaphthalene. Agency for Toxic Substances and Disease Registry, Atlanta, GA, p. 8.

Baumard, P., Budzinski, H., Garrigues, P., Dizer, H., Hansen, P.D., 1999. Polycyclic aromatic hydrocarbons in recent sediments and mussels (Mytilus edulis) from the Western Baltic Sea: occurrence, bioavailability and seasonal variations. Mar. Environ. Res. 47, 17–47.

CEMP, 2009. CEMP Assessment Report 2008/2009. Assessment of Trends and Concentrations of Selected Hazardous Substances in Sediments and Biota. OSPAR Commission https://oap.ospar.org/en/ospar-assessments/intermediate-assessment-2017/pressures-human-activities/contaminants/pah-sediment/ (2020-03-10).

Conde, F.J., Ayala, J.H., Afonso, A.M., González, V., 2005. Emissions of polycyclic aromatic hydrocarbons from combustion of agricultural and sylvicultural debris. Atmos. Environ. 39, 6654–6663.

Cornelissen, G., Gustafsson, Ö., Bucheli, T.D., Jonker, M.T.O., Koelmans, A.A., van Noort, P.C.M., 2005. Extensive sorption of organic compounds to black carbon, coal, and Kerogen in sediments and soils: mechanisms and consequences for distribution, bioaccumulation, and biodegradation. Environ. Sci. Technol. 39, 6881–6895.

Deng, W., Li, X.G., Li, S.Y., Ma, Y.Y., Zhang, D.H., 2013. Source apportionment of polycyclic aromatic hydrocarbons in surface sediment of mud areas in the East China Sea using diagnostic ratios and factor analysis. Mar. Pollut. Bull. 70, 266–273.

Guo, Z., Lin, T., Zhang, G., Yang, Z., Fang, M., 2006. High-resolution depositional records of polycyclic aromatic hydrocarbons in the central continental shelf mud of the East China Sea. Environ. Sci. Technol. 40, 5304–5311.

Jenkins, B.M., Jones, A.D., Turn, S.Q., Williams, R.B., 1996. Emission factors for polycyclic aromatic hydrocarbons from biomass burning. Environ. Sci. Technol. 30, 2462–2469.

Jiao, W., Wang, T., Khim, J.S., Luo, W., Hu, W., Naile, J.E., Giesy, J.P., Lu, Y., 2012. PAHs in surface sediments from coastal and estuarine areas of the northern Bohai and Yellow Seas, China. Environ. Geochem. Hlth. 34, 445–456.

Johannesson, K., Andre, C., 2006. Life on the margin: genetic isolation and diversity loss in a peripheral marine ecosystem, the Baltic Sea. Mol. Ecol. 15, 2013–2029.

Khalili, N.R., Scheff, P.A., Holsen, T.M., 1995. PAH source fingerprints for coke ovens, diesel and, gasoline engines, highway tunnels, and wood combustion emissions. Atmos. Environ. 29, 533–542.

Kim, K.H., Jahan, S.A., Kabir, E., Brown, R.J., 2013. A review of airborne polycyclic aromatic hydrocarbons (PAHs) and their human health effects. Environ. Int. 60, 71–80.

Larsen, R.K., Baker, J.E., 2003. Source apportionment of polycyclic aromatic hydrocarbons in the urban atmosphere: a comparison of three methods. Environ. Sci. Technol. 37, 1873–1881.

Levendis, Y.A., Atal, A., Carlson, J.B., 1998. On the correlation of CO and PAH emissions from the combustion of pulverized coal and waste tires. Environ. Sci. Technol. 32, 3767–3777.

Li, J., Dong, H., Zhang, D., Han, B., Zhu, C., Liu, S., Liu, X., Ma, Q., Li, X., 2015. Sources and ecological risk assessment of PAHs in surface sediments from Bohai Sea and northern part of the Yellow Sea, China. Mar. Pollut. Bull. 96, 485–490.

Li, J., Dong, H., Xu, X., Han, B., Li, X., Zhu, C., Han, C., Liu, S., Yang, D., Xu, Q., Zhang, D., 2016. Prediction of the bioaccumulation of PAHs in surface sediments of Bohai Sea, China and quantitative assessment of the related toxicity and health risk to humans. Mar. Pollut. Bull. 104, 92–100.

Lin, T., Hu, L., Guo, Z., Qin, Y., Yang, Z., Zhang, G., Zheng, M., 2011. Sources of polycyclic aromatic hydrocarbons to sediments of the Bohai and Yellow Seas in East Asia. J. Geophys. Res. Atmos. 116 (D23).

Lin, Y., Deng, W., Li, S., Li, J., Wang, G., Zhang, D., Li, X., 2017. Congener profiles, distribution, sources and ecological risk of parent and alkyl-PAHs in surface sediments of Southern Yellow Sea, China. Sci. Total Environ. 580, 1309–1317.

Liu, Y., Chen, L., Huang, Q.-h., Li, W.-y., Tang, Y.-j., Zhao, J.-f., 2009. Source apportionment of polycyclic aromatic hydrocarbons (PAHs) in surface sediments of the Huangpu River, Shanghai, China. Sci. Total Environ. 407, 2931–2938.

Louvado, A., Gomes, N.C.M., Simões, M.M.Q., Almeida, A., Cleary, D.F.R., Cunha, A., 2015. Polycyclic aromatic hydrocarbons in deep sea sediments: microbe–pollutant interactions in a remote environment. Sci. Total Environ. 526, 312–328.

Lubecki, L., Kowalewska, G., 2010. Distribution and fate of polycyclic aromatic hydrocarbons (PAHs) in recent sediments from the Gulf of Gdańsk (SE Baltic). Oceanologia 52 (4).

Mai, B., Qi, S., Zeng, E.Y., Yang, Q., Zhang, G., Fu, J., Sheng, G., Peng, P., Wang, Z., 2003. Distribution of polycyclic aromatic hydrocarbons in the coastal region off Macao, China: assessment of input sources and transport pathways using compositional analysis. Environ. Sci. Technol. 37, 4855–4863.

Maletić, S.P., Beljin, J.M., Rončević, S.D., Grgić, M.G., Dalmacija, B.D., 2019. State of the art and future challenges for polycyclic aromatic hydrocarbons is sediments: sources, fate, bioavailability and remediation techniques. J. Hazard. Mater. 365, 467–482.

Marr, L.C., Kirchstetter, T.W., Harley, R.A., Miguel, A.H., Hering, S.V., Hammond, S.K., 1999. Characterization of polycyclic aromatic hydrocarbons in motor vehicle fuels and exhaust emissions. Environ. Sci. Technol. 33, 3091–3099.

Mi, L., Xie, Z., Zhao, Z., Zhong, M., Mi, W., Ebinghaus, R., Tang, J., 2019. Occurrence and spatial distribution of phthalate esters in sediments of the Bohai and Yellow seas. Sci. Total Environ. 653, 792–800.

Norris, G., Duvall, R., Brown, S., Bai, S., 2014. EPA Positive Matrix Factorization (PMF) 5.0 Fundamentals and User Guide. U.S. Environmental Protection Agency, Washington, DC, p. 20460.

OSPAR, 2010. Quality Status Report 2010. OSPAR commission, London https://qsr2010.ospar.org/en/index.html (2020-03-10).

OSPAR, 2017. MIME Regional Assessment of Status and Trends in PAH Concentrations in Sediment. http://dome.ices.dk/osparmime2016/regional_assessment_sediment_pah_(parent).html.

Otte, J.C., Keiter, S., Faßbender, C., Higley, E.B., Rocha, P.S., Brinkmann, M., Wahrendorf, D.-S., Manz, W., Wetzel, M.A., Braunbeck, T., Giesy, J.P., Hecker, M., Hollert, H., 2013. Contribution of priority PAHs and POPs to Ah receptor-mediated activities in sediment samples from the River Elbe Estuary, Germany. PLoS One 8, e75596.

Porta, M., 2015. Human contamination by persistent toxic substances: the rationale to improve exposure assessment. Environ. Sci. Pollut. Res. Int. 22, 14560–14565.

Qiao, S., Shi, X., Wang, G., Zhou, L., Hu, B., Hu, L., Yang, G., Liu, Y., Yao, Z., Liu, S., 2017. Sediment accumulation and budget in the Bohai Sea, Yellow Sea and East China Sea. Mar. Geol. 390, 270–281.

Ricking, M., Schulz, H.M., 2002. PAH-profiles in sediment cores from the Baltic Sea. Mar. Pollut. Bull. 44, 565–570.

Soliman, Y.S., Al Ansari, E.M.S., Wade, T.L., 2014. Concentration, composition and sources of PAHs in the coastal sediments of the exclusive economic zone (EEZ) of Qatar, Arabian Gulf. Mar. Pollut. Bull. 85, 542–548.

Song, S., Ruan, T., Wang, T., Liu, R., Jiang, G., 2014. Occurrence and removal of benzotriazole ultraviolet stabilizers in a wastewater treatment plant in China. Environ. Sci-Proc. Imp. 16, 1076–1082.

SRU, 2004. Marine Environment Protection for the North and Baltic Seas: Special Report. https://www.umweltrat.de/SharedDocs/Downloads/EN/02_Special_Reports/2004_Special_Report_Marine_Environment_Protection_Summary.html (2020-03-10).

Tobiszewski, M., Namieśnik, J., 2012. PAH diagnostic ratios for the identification of pollution emission sources. Environ. Pollut. 162, 110–119.

Wang, M., Wang, C., Hu, X., Zhang, H., He, S., Lv, S., 2015. Distributions and sources of petroleum, aliphatic hydrocarbons and polycyclic aromatic hydrocarbons (PAHs) in surface sediments from Bohai Bay and its adjacent river, China. Mar. Pollut. Bull. 90, 88–94.

Wang, P., Zhang, Q., Li, Y., Matsiko, J., Zhang, Y., Jiang, G., 2017. Airborne persistent toxic substances (PTSs) in China: occurrence and its implication associated with air pollution. Environ. Sci-Proc. Imp. 19, 983–999.

Wolska, L., Mechlińska, A., Rogowska, J., Namieśnik, J., 2012. Sources and fate of PAHs and PCBs in the marine environment. Crit. Rev. Env. Sci. Tec. 42, 1172–1189.

Xu, Y., Liu, T., Zhu, X., Ji, G., 2019. Quantitative analysis of genetic associations in the biodegradative pathway of PAHs in wetland sediments of the Bohai coast region. Chemosphere 218, 282–291.

Yan, B., Abrajano, T.A., Bopp, R.F., Chaky, D.A., Benedict, L.A., Chillrud, S.N., 2005. Molecular tracers of saturated and polycyclic aromatic hydrocarbon inputs into Central Park Lake, New York City. Environ. Sci. Technol. 39, 7012–7019.

Yang, Z.S., Liu, J.P., 2007. A unique Yellow River-derived distal subaqueous delta in the Yellow Sea. Mar. Geol. 240, 169–176.

Yang, C., Lambert, P., Zhang, G., Yang, Z., Landriault, M., Hollebone, B., Fieldhouse, B., Mirnaghi, F., Brown, C.E., 2017. Characterization of chemical fingerprints of unconventional Bakken crude oil. Environ. Pollut. 230, 609–620.

Zhang, R., Li, T., Russell, J., Zhang, F., Xiao, X., Cheng, Y., Liu, Z., Guan, M., Han, Q., 2020. Source apportionment of polycyclic aromatic hydrocarbons in continental shelf of the East China Sea with dual compound-specific isotopes (δ13C and δ2H). Sci. Total Environ. 704, 135459.

Zhao, X., Jin, H., Ji, Z., Li, D., Kaw, H.Y., Chen, J., Xie, Z., Zhang, T., 2020. PAES and PAHs in the surface sediments of the East China Sea: occurrence, distribution and influence factors. Sci. Total Environ. 703, 134763.